

Endocytosis Controls Spreading and Effective Signaling Range of Fgf8 Protein

Steffen Scholpp^{1,2} and Michael Brand^{1,*}

¹Max Planck Institute of Molecular Cell Biology and Genetics and Department of Genetics Dresden University of Technology D-01307 Dresden Germany

Summary

Secreted signaling molecules released from a restricted source are of great importance during embryonic development because they elicit induction, proliferation, differentiation, and patterning events in target cells [1, 2]. Fgf8 is a member of the fibroblast growth factor family with key inductive functions during vertebrate development of, for example, the forebrain [3], midbrain [4], cerebellum [5], heart [6], inner ear [7], and mesoderm [8]. However, the mechanism by which the signaling range of Fgf8 is controlled in a field of target cells is unknown. We studied Fgf8 as a potential morphogen in the nascent neuroectoderm of living zebrafish embryos. We find that spreading of epitope-tagged Fgf8 through target tissue is carefully controlled by endocytosis and subsequent degradation in lysosomes, or “restrictive clearance,” from extracellular spaces. If internalization is inhibited, Fgf8 protein accumulates extracellularly, spreads further, and activates target gene expression over a greater distance. Conversely, enhanced internalization increases Fgf8 uptake and shortens its effective signaling range. Our results suggest that Fgf8 spreads extracellularly by a diffusion-based mechanism and demonstrate that target cells can actively influence, through endocytosis and subsequent degradation, the availability of Fgf8 ligand to other target cells.

Results and Discussion

To determine how Fgf8 spreads through tissue, we fluorescently labeled recombinantly manufactured zebrafish Fgf8 protein in vitro with Cy3 chromophore [9] and monitored spreading of Fgf8 protein from a focal source in developing zebrafish embryos. Labeled Fgf8 protein retains its biological function and spreads differently from residual, uncoupled dye (see the Supplemental Data available with this article online). We implanted Heparin beads coated with Fgf8-Cy3 at the animal pole at the 30% epiboly stage, as described previously [6]. At different hours post implantation (hpi), we analyzed spreading of the labeled protein through the forming neuroectoderm by laser scanning confocal microscopy in living embryos (Figure 1). After 1, 2, and 3 hpi, Fgf8-

Cy3 protein accumulates in intracellular vesicles at 4, 8, and 12 cell diameters away from the source, respectively (Figures 1A, 1D, and 1G). In parallel experiments, we find that the Fgf8 target gene *sprouty4* (*spry4*) [10] is induced around the implanted beads in such embryos, at a distance of 8, 13, and 16 cells away from the source (Figures 1B, 1E, and 1H). To determine if movement of cells exposed to Fgf8-Cy3 contributes to propagation of the protein, we implanted labeled cells and tracked them over the same period (Figures 1C, 1F, and 1I). After 3 hpi of monitoring their movement, cells can spread over a distance of about 3 cells (Figure 1I), whereas vesicular protein is detected up to a distance of 16 cells. Therefore, Fgf8-Cy3 protein can spread through tissue away from an artificial source over time, in a manner that correlates with target gene induction but not with cell movement. In target cells, Fgf8-Cy3 accumulates in intracellular vesicles, allowing us to estimate a minimum rate of spreading of about 5 cells/hr through tissue (Figure 1J).

To understand the mechanism by which Fgf8 moves through tissue, we sought the identity of the intracellular compartment(s) in target cells that contain labeled Fgf8. Small GTPases of the Rab family both label and functionally define organelle types by recruiting the vesicle tethering and fusion machinery to specific subcellular organelles [11]. Rab5 proteins in particular mark clathrin-coated vesicles that bud off the plasma membrane and fuse with the early endosome [12, 13], and Rab5 protein level and activity are critical for controlling trafficking through the early endosome. Two zebrafish Rab5 genes show high homology with the mammalian isoforms Rab5a and Rab5c. In cell culture, all three Rab5 isoforms (a–c) share all structural features required for regulation of endocytosis and are functionally redundant [12]. In confocal movies of embryos subjected to a classical in vivo fluid-phase uptake experiment with rhodamine dextran, we find that a fusion protein of zebrafish Rab5a:YFP colocalizes with dextran and is observed in small and large vesicles [14] (see Supplemental Data). Next, we implanted Fgf8-Cy3-coated beads into embryos injected with *rab5:YFP* mRNA. In these embryos, Fgf8-Cy3 and Rab5:YFP are colocalized in 54% of the Fgf8-positive vesicles ($n = 29$ of 54; Figures 2A–2A’), suggesting that Fgf8 is taken up by target cells and transported to early endosomes. Some Fgf8-positive vesicles do not colocalize with Rab5:YFP, which we assume reflects further transport of the protein along the endosomal pathway, for example to lysosomes (see below).

Next we asked how altering the rate of endocytosis by various regimens would influence Fgf8 protein propagation through Fgf8-receiving tissue of host embryos. In these experiments, instead of Heparin beads, we transplanted small groups of cells expressing Myc-tagged Fgf8 through the secretory pathway to the animal pole of host embryos. Host embryos furthermore carried a Histone2A:GFP transgene (H2A:GFP) [15] to aid localization of Fgf8:Myc protein within the tissue. Two hours

*Correspondence: brand@mpi-cbg.de

²Present address: Medical Research Council Centre for Developmental Neurobiology, King’s College London, New Hunt’s House, 4th Floor, Guy’s Hospital Campus, London SE1 1UL, England.

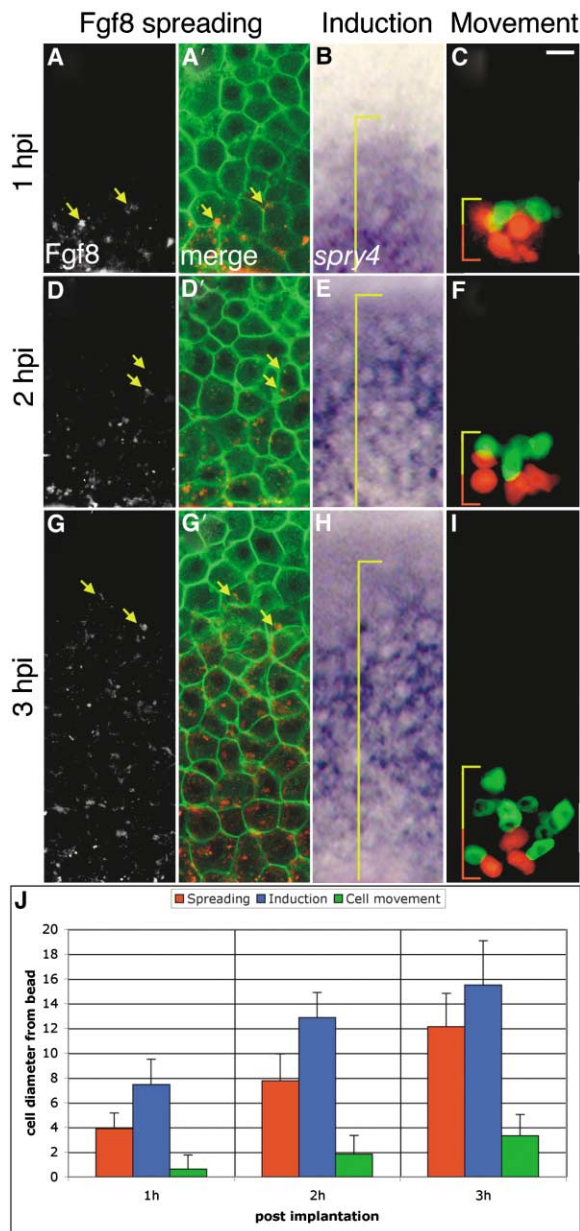


Figure 1. Spreading of Fgf8 Protein and Target Gene Induction
(A)–(I) show living zebrafish embryos, animal pole view. Fgf8-Cy3-coated beads were implanted at the animal pole at sphere stage and, up to 3 hr post implantation (hpi), propagation of Fgf8 was analyzed in living embryos by visualizing the protein spreading with confocal microscopy (black and white images [A], [D], and [G]) and in superimposed images with a Bodipy-ceramide C5 counterstaining [37] for the ECM (A', D', and G'). The position of the bead is one cell row further down and is not shown because of the high intensity. After 1, 2, and 3 hpi, we found Fgf8 positive vesicles mainly intracellularly localized, detected 3.9 (± 1.3), 7.8 (± 2.2), and 12.1 (± 2.7) cell diameters away from the implanted bead ($n = 9$). In (B), (E), and (H), we monitored the expression of *sprouty4* and found induction of the target gene 7.5 (± 2.0), 12.9 (± 2.0), and 15.5 (± 3.6) cells away from the source ($n = 10$). Induction is observed over a slightly wider range than vesicular protein in this assay, presumably because Fgf8 protein signals are already at concentrations that are too low to detect. Gastrulation movements of the tissue (C, F, and I) were monitored by transplantation of labeled donor cells marked by rhodamine dextran or fluorescein isothiocyanate (FITC)-coupled dex-

post transplantation (hpt), embryos were fixed at the 60% epiboly stage, and Fgf8:MyC protein was detected by immunocytochemistry. In embryos with normal endocytosis, Fgf8:MyC was localized in vesicular structures within the receiving cells at a maximum distance of 9 cells from the source (Figures 2B and 2B'), similar to the case of Fgf8-Cy3. We detect Fgf8 only after it accumulates in vesicles (Figures 2B and 2B'), probably because of its low concentration in the extracellular matrix (ECM). In the host embryos, we altered the rate of internalization by interfering with receptor internalization, down-regulating or stimulating the endocytic pathway, or blocking vesicle fission. Internalization was decreased by injecting a dominant-negative, mutated form of the Fgf receptor XFD [16], which lacks the intracellular tyrosine kinase domain required for receptor-mediated internalization [17, 18]. Instead of the intracellular localization of Fgf8 observed in wild-type siblings, host embryos injected with XFD mRNA show an accumulation of Fgf8:MyC protein in a “honeycomb” pattern around the receiving cells (Figures 2C and 2C'; $n = 8$ embryos examined), reflecting the extracellular accumulation of Fgf8. Furthermore, Fgf8 protein is observed at greater distances from the source than in uninjected control embryos (Figures 2B and 2C; 15 cells away from source after 2 hr, compared to 9 cells in control embryos; $n = 6$). To determine if endocytosis is required for Fgf8 uptake, we inactivated Rab5 function by injecting RN-tre, a GTPase-activating-protein that specifically acts on Rab5; it converts it into the inactive Rab5-GDP form [19], thus down-regulating Rab5-dependent endocytosis. Similar to XFD-misexpressing host embryos, Fgf8 was absent from intracellular vesicles and accumulated extracellularly at a greater distance from the source (Figures 2D and 2D').

In the converse experiment, we stimulated internalization by injecting 200 pg zebrafish *rab5a* or *rab5c* RNA into the host embryos. Compared to that of uninjected wild-type siblings, the range of Fgf8:MyC spreading was reduced in embryos overexpressing Rab5, and the size of Fgf8-positive compartments was increased (Figures 2E and 2E', diagrams), as described previously for early endosomes in tissue culture cells [20]. These results show that Fgf8 is taken up via Rab5-dependent endocytosis and that Rab5 activity and endocytosis can influence the range of Fgf8 protein spreading through tissue. Therefore, we propose that changing the rate of internalization by the endocytic pathway strongly influences Fgf8 propagation. Next, we tested whether small cell clones with altered Rab5-dependent internalization levels could equally interfere with propagation of Fgf8. Donor embryos were coinjected with 250 pg RN-tre mRNA and a membrane bound form of GFP (mem-GFP) as a

tran. At sphere stage, small cell clones containing 3–5 cells from both donors were transplanted into an unlabeled host embryo. After 1, 2, and 3 hpi, the cells spread over a distance of 0.6 (± 1.1), 1.8 (± 1.5), and 3.3 (± 1.7) cells ($n = 13$). (J) Spreading of Fgf8 protein (red bars), induction of *sprouty4* (blue bars), and cell spreading (green bars) are depicted over 3 hpi; the arrow bars show standard deviation. The scale bar represents 15 μ m (C).

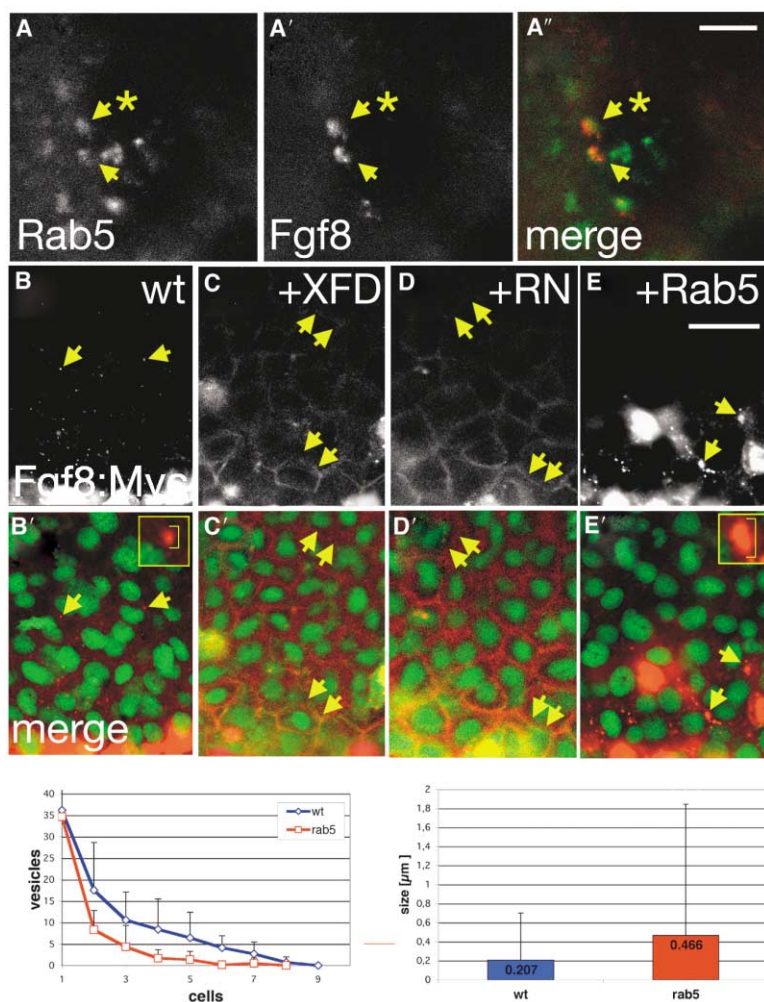


Figure 2. Fgf8 Protein Spreading Is Influenced by Internalization

(A) Fgf8-Cy3 is located in early endosomes, marked by injection of 150 pg *rab5a:YFP* mRNA. After implantation of Fgf8-Cy3-coated beads, labeled protein (A') colocalizes with Rab5 (A', yellow arrows). The asterisk marks the location of the nucleus.

(B–E') Donor embryos were injected with Fgf8:Myc, and rhodamine dextran was used as lineage tracer. Cell clones from these embryos were transplanted into host embryos injected with different mRNAs. After 2.5 hpi, embryos were fixed prior to α -Myc antibody staining and confocal analysis.

A transgenic line carrying an H2A:GFP transgene was used to visualize the nuclei. In wild-type siblings, the vesicles in the target cells stain with Fgf8:Myc, whereas the transplanted donor cells are marked additionally by the lineage tracer (B). (B') is a merged image. In (B) and (B'), Fgf8 was localized in vesicles in the receiving cells marked with yellow arrows. Embryos were injected with 200 pg mRNA encoding a dominant-negative Fgf receptor (XFD; [C] and [C']) or with 250 pg *RN-tre* mRNA (D and D'). Fgf8 accumulated in an extracellular "honeycomb" pattern (double arrows). Intracellular Fgf8 staining was strongly decreased. In contrast, stimulating endocytosis through injection of 250 pg *rab5* mRNA reduced Fgf8 protein spreading, yielding bigger vesicles in the cells directly adjacent to the source ([E] and E'), marked with arrows; the accession numbers for Rab5a and Rab5c are BC049057 and BC045466, respectively). The small panels in the upper right corner of (B') and (E') show examples of vesicles at higher magnification. Comparison of wild-type siblings to embryos overexpressing Rab5a shows that the number of vesicles in the first cell row adjacent to the source is similar ($n = 35$ and $n = 36$), whereas

in the second cell row and beyond, a significant decrease in vesicle number was found. After six cell rows, hardly any vesicles are detected ($n = 306$). In wild-type embryos, Fgf8-positive vesicles were $0.21 \mu\text{m}$ in diameter (± 0.46 ; $n = 607$), whereas Rab5-overexpressing embryos contained vesicles of $0.47 \mu\text{m}$ (± 1.34 ; $n = 306$; $p = 0.001$). Method: Vesicle numbers were determined with an algorithm of the National Institutes of Health image derive ImageJ version 1.29, set to detect a threshold size of greater than $0.1 \mu\text{m}$.

in the second cell row and beyond, a significant decrease in vesicle number was found. After six cell rows, hardly any vesicles are detected ($n = 306$). In wild-type embryos, Fgf8-positive vesicles were $0.21 \mu\text{m}$ in diameter (± 0.46 ; $n = 607$), whereas Rab5-overexpressing embryos contained vesicles of $0.47 \mu\text{m}$ (± 1.34 ; $n = 306$; $p = 0.001$). Method: Vesicle numbers were determined with an algorithm of the National Institutes of Health image derive ImageJ version 1.29, set to detect a threshold size of greater than $0.1 \mu\text{m}$.

lineage tracer (Figure 3A) [21]. At dome stage, small cell clones were transplanted from the injected embryo into a position close to the endogenous expression domain of Fgf8 of a host embryo transgenic for H2A:GFP (Figure 3A'). After transplantation, an Fgf8-Cy3-coated bead was implanted into the embryo (Figure 3A'). After 2 hpi, the embryo was mounted and analyzed by confocal microscopy in vivo (Figure 3A''). Because of the lineage tracer and the transgenic background, RN-tre-injected, transplanted cells have stained membranes and nuclei, whereas host cells have only stained nuclei (Figure 3B). After implantation, Fgf8 is released from the bead and accumulates in wild-type cells, whereas RN-tre-injected cells fail to internalize Fgf8 (Figures 3B' and 3B''). Host cells took up the protein even if cells inhibited for Rab5 function were located between the source and the receiving cells (Figure 3B''). Although difficult to quantitate, it appears that between the cells of the clone, little extracellular Fgf8 accumulates, unlike in tissue in which all cells exhibit reduced internalization rates (Figures 2C–2D'). Because the surrounding wild-type cells take up

Fgf8 normally, we tentatively suggest that this prevents the buildup of high levels of extracellular Fgf8 protein in the area of the clone itself.

In a similar approach, we overexpressed Rab5 in the transplanted cells marked by mem-GFP (Figures 3C–3C''). The observed phenotype was now exactly the opposite: Rab5-overexpressing clones accumulate Fgf8, and larger vesicles are observed in the clone (Figures 3C' and 3C''). In addition, cells that lie behind the clone (relative to the source of Fgf8) now appear deficient for Fgf8 protein ("shadow," Figure 3C''). In *Drosophila*, spreading of the TGF- β ligand Dpp is thought to occur by planar transcytosis, a process that requires endocytosis [22, 23]. Dpp spreading is enhanced by overexpressing Rab5, whereas a clone with reduced endocytic activity acts like a barrier and creates a shadow behind it [22]. Although endocytosis is important for both types of morphogens, our experiments suggest that, unlike the case of Dpp, transcytosis plays little or no part in the propagation of Fgf8.

In the next series of experiments, we asked how alter-

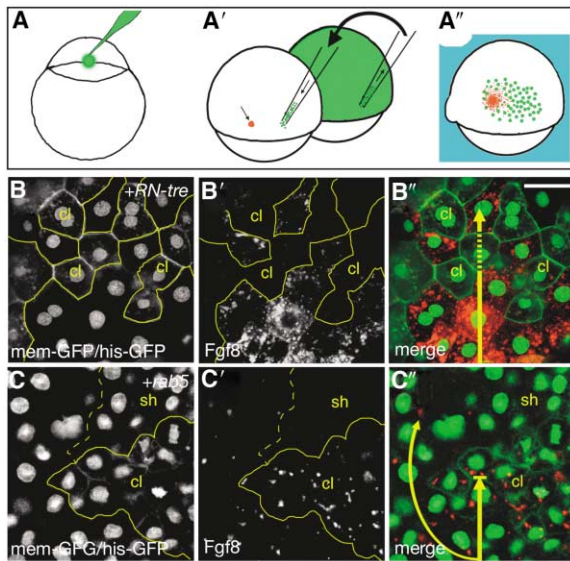


Figure 3. Properties of Cell Clones with Altered Internalization
Donor embryo cells injected with 250 pg *RN-tre* mRNA and 50 pg mem-GFP (A) were transplanted into wild-type host embryos, and a bead coated with Fgf8-Cy3 was implanted adjacent to the clone (A'). At 2 hpi, embryos were embedded into LMP agarose (blue square) and analyzed by confocal microscopy *in vivo* (A''). The mem-GFP served as lineage tracer (B and C). All cells carry the H2A:GFP transgene for visualization of the nuclei. Cells with reduced endocytosis have a strongly reduced ability to internalize Fgf8 (surrounded by yellow line and marked with “cl”), as shown in (B') and in the superimposed image (B''). In contrast, when transplanted cells were derived from donors injected with 250 pg *rab5* mRNA to stimulate endocytosis, Fgf8 accumulated in the grafted cells [(C' and C''); cells are marked by a solid line surrounding the clone, “cl”). Few Fgf8 vesicles are detected behind the clone; they form a “shadow” [(C' and C''); marked with dashed lines and “sh”). The yellow arrow indicates the potential direction of movement of Fgf8 away from the source. The scale bar represents 15 μ m.

ing endocytosis affects signaling to Fgf8 target genes (Figure 4). Reducing endocytosis does not affect the expression of Fgf8 mRNA in source cells. At 70% epiboly, endogenous Fgf8 is expressed in about eight rows of cells at the blastoderm margin, a tissue that later gives rise to the mesodermal and endodermal germ layers (Figure 4B) [5, 24]. The Fgf8 target genes *spry4* [10], *erm*, and *pea3* [25, 26] are expressed in successively broader domains: *spry4* in about 13 cell rows (Figure 4D); *pea3* in about 15 cell rows (Figure 4B); and *erm* in about 17 cell rows (Figure 4C). Comparison of *fgf8* expression with target gene expression therefore suggests that Fgf8 protein can signal over a distance of at least 9 cells and, in addition, is able to trigger different responses (Figure 4P).

We then examined how decreased endocytosis affects signaling to activate Fgf8 target genes (Figures 4E–4H). We found that expression of target genes was broadened in both germ layers, whereas *fgf8* expression at the source was barely changed. In *RN-tre*-mRNA-injected embryos, Fgf8 expression was slightly increased, from eight to ten cell rows (Figure 4E). Importantly, *pea3* was induced in 23 cell rows (Figure 4F), *erm* in 29 cell rows (Figure 4G), and *spry4* in 37 cell rows

and often throughout the embryo at increased levels and in a much broader domain than in embryos with normal levels of Rab5 activity (Figure 4H). Notably, both in wild-type embryos and when endocytosis is reduced, the expression of the target genes *erm*, *pea3*, and *spry4* is nested relative to the source of Fgf8. Curiously, compared to *erm* and *pea3*, *spry4* shows the most narrow expression domain in wild-type embryos (Figures 4B–4D) but is most sensitive in its response to Fgf8 when internalization is suppressed (Figure 4H). Additional factors may therefore contribute to activation of these genes, or secondary, dosage-sensitive interactions might occur between *spry4* and the *ets* factors, *erm* and *pea3*. Also, the two inhibitory processes controlling Fgf8 signaling—endocytic clearance of the activated ligand-receptor complex and repression of the MAPK pathway by *Spry4*, respectively—might be linked, in which case internalization could inhibit the expression of *spry4* more directly. Although the detailed mechanisms are not clear yet, we observe that target genes respond to different concentrations of Fgf8 protein, raising the possibility that Fgf8 has properties similar to a morphogen and that endocytosis might contribute to shaping the response of the embryo to Fgf8 (Figure 4P).

Apart from regulating the activity state of Rab5, *RN-tre* is also involved in epidermal growth factor (EGF) signaling [19], which, like Fgf signaling, employs the MAPK pathway, raising the possibility that widespread *spry4* expression might result from a possible crossactivation through the EGF pathway. Therefore, as a control, we determined whether the widespread *spry4* response still requires Fgf ligand by injecting mRNA encoding XFD (Figure 4I) or XFD and *RN-tre* (Figure 4J). In these embryos, *spry4* expression was strongly suppressed, showing that the observed widespread target gene induction is closely dependent on Fgf receptor-mediated signaling. Furthermore, control embryos injected with *RN-tre* mRNA and treated with a small-molecule inhibitor of Fgf receptor kinase activity (SU5402) [27] showed no *spry4* induction, whereas *fgf8* expression is not altered (not shown). Also, injection of a nonfunctional *RN-tre* variant with a mutation in the GAP domain (D147A) [19] has no effect on *spry4* expression (Figure 4K).

The above results suggest that endocytosis is required to restrict the range of cells responding to an Fgf8 source. To test this notion further, we blocked fission of clathrin-coated vesicles from the plasma membrane with a dominant-negative variant of Dynamin2 GTPase (Dyn2-K44A) [28]. Overexpression of wild-type *dyn2* caused no expansion of target gene expression (Figure 4L). In contrast, injecting *Dyn2-K44A* mRNA causes a strong expansion of *spry4*, *pea3*, and *erm* expression toward the animal pole (Figure 4M; Supplemental Data); this expansion can be blocked with SU5402 inhibitor, again confirming that this phenotype is dependent on functional Fgf receptor (Figure 4N). Next, we sought to specifically knock down Rab5-dependent endocytosis. We injected morpholino-antisense oligonucleotides (MO) that specifically block the translation of Rab5a, which resulted in a broadened expression of *spry4* (Figure 4O). In control experiments, the specificity of the *rab5a* MO was confirmed by coinjecting a noninhibitable form of *rab5a* mRNA that lacks

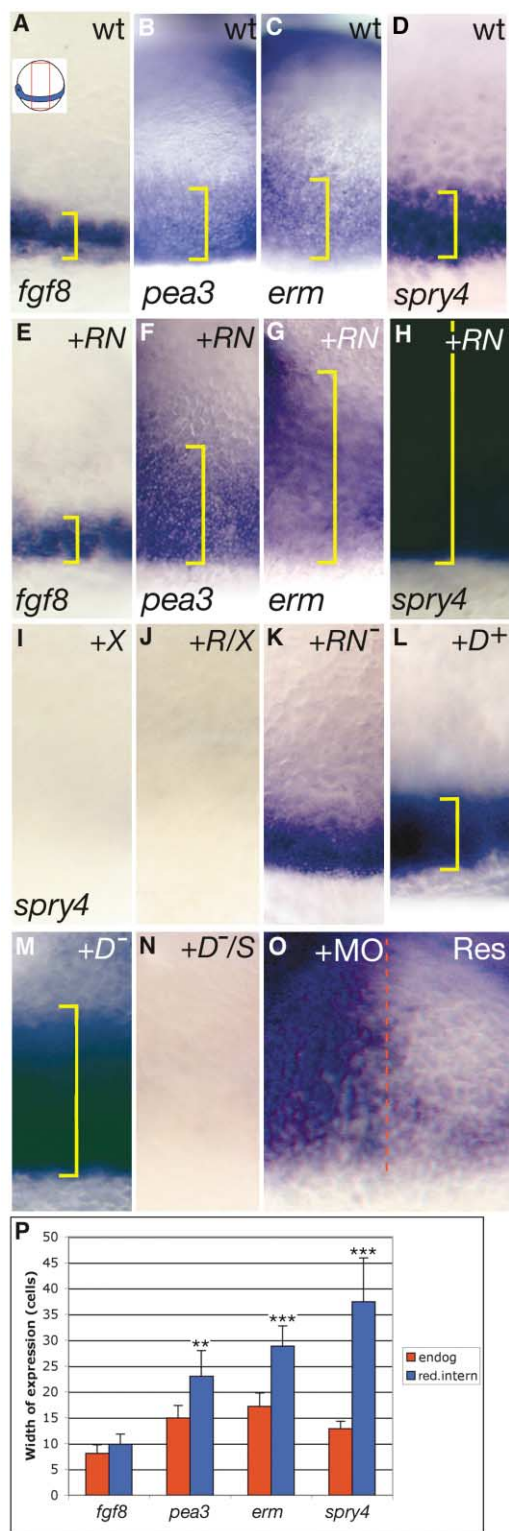


Figure 4. Decreased Internalization Expands Effective Signaling Range

Images show the lateral part of embryos after in situ hybridization with the indicated probes at 70% epiboly ([A], small image in the upper left corner; the dorsal shield organizer is marked by an asterisk). Panels (A)–(N) show a lateral embryo view oriented animal to the top, and (O) shows a frontal view.

the MO binding site into one of two blastomeres (Figure 4O).

To explore further the relationship between endocytosis and Fgf8 activity, we stimulated endocytosis at various levels by injecting different concentrations of *rab5a* mRNA. Injected embryos also received a bead coated with a constant amount of Fgf8 protein at the animal pole and implanted at 30% epiboly (Figure 5). In control siblings, *spry4* target gene induction was observed around the bead at a width of 16 cells after 3 hpi (Figures 5A and 5D). In embryos injected with 125 pg and 250 pg *rab5a* RNA, the induction of *spry4* was severely decreased, to a width of 11 cells and 8 cells, respectively (Figures 5B–5D). Thus, normal levels of endocytosis are evidently not needed for Fgf8 signaling to occur. Instead, we suggest that endocytosis serves to *restrict* spreading of Fgf8 protein away from the source, by *clearing* Fgf8 protein from the extracellular space (ECS) of target tissue (the “restrictive clearance model”). In this model, the level of endocytosis influencing the extracellular concentration of Fgf8 is a key determinant defining how far the protein is allowed to spread and, thus, determining the width of the target tissue responding to Fgf8 signaling.

The restrictive clearance model makes several important, testable predictions. One prediction is that target cells might contribute to decreasing the amount of Fgf8 present in extracellular space, for instance by degrading Fgf8 protein after internalization. Immunoelectron microscopy (EM) indeed detects Fgf8 in receiving cells in the degradative pathway, for example in early endosomes and lysosomes (Figure 6). Three hours after transplantation, embryos containing an Fgf8:Myc-expressing clone were fixed and processed for Fgf8:Myc detection in cells adjacent to the implanted clone (Figure 6A, arrowheads). The transplanted donor cells were identified

(A) Fgf8 is expressed in a domain 8.1 cells \pm 1.7 (n = 8) wide. (B–D) Expression of the Fgf target genes *pea3*, *erm*, and *spry4* at the same stage, in broader domains with widths of 14.9 \pm 2.4 (n = 11), 17.2 \pm 2.6 (n = 10), and 15.6 \pm 2.2 (n = 12) cells, respectively. Injection of 250 pg *RN-tre* mRNA has only a minor effect on *fgf8* expression (9.9 cells \pm 1.9; n = 8; [E]). In contrast, target gene expression is strongly expanded toward the animal pole when internalization is decreased (*pea3*: 23.0 cells \pm 5.0, n = 8; *erm*: 28.8 cells \pm 3.9, n = 6; and *spry4*: 37.4 cells \pm 8.5, n = 7; [F–H]). Controls: Injection of 200 pg *XFD* mRNA reduces Fgf signaling in wild-type embryos (I) and *RN-tre*-misexpressing embryos (J); the nonfunctional *RN-tre* D147A variant has no effect on *spry4* expression (K). (L–N) Blocking dynamin2 function. Injection of 300 pg mRNA encoding the dominant-negative dynamin2 (K44A) variant caused a strong expansion of *spry4* (M), whereas the wild-type form causes no phenotype (L). Treatment of embryos injected with *dyn2-K44A* mRNA with 16 μ m SU5402 revealed a strict dependency on Fgfr signaling (N). (O) Morpholino knock-down of Rab5a function. Injection of 2 ng *rab5a*-MO (+MO) causes a similar phenotype to that shown in (H). Coinjection rescue by a nonblockable *rab5a* mRNA lacking the MO binding site into one half of the embryo demonstrates the specificity of the *rab5a* MO ([O], Res).

(P) Width of target gene expression at normal (red) and reduced (blue) Fgf8 internalization rates. Error bars show standard deviation and “**” or “***” mark a significant difference between the injected embryos and the control embryos, with a confidence interval of α = 0.05 or α = 0.001.

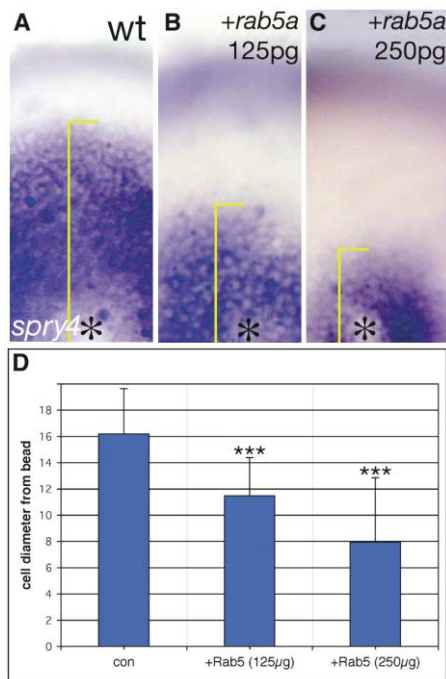


Figure 5. Increased Internalization Reduces Effective Signaling Range

At 30% epiboly, implantation of an Fgf8-coated bead at the animal pole caused induction of *spry4* in a halo around the implantation site. In control embryos, we observed target gene induction around the bead at a width of 16.2 (± 3.4) cells after 3 hpi (A and D). After injection with 125 pg and 250 pg *rab5a* RNA, the induction of *spry4* was severely decreased to a width of 11.4 cells (± 2.9) and 7.9 cells (± 4.9 ; [B–D]), respectively. (D) shows the relation between *spry4* induction and *rab5a* misexpression levels. Error bars show standard deviation, and “***” marks a highly significant difference between injected and control embryos, with a confidence interval of $\alpha = 0.001$.

by strong labeling of the trans-Golgi network (not shown). In target cells, we identified Fgf8:Myc in several intracellular compartments with the typical morphology [29] of early endosomes (Figures 6A and 6A'), late endosomes or multivesicular bodies (Figure 6A''), and lysosomes containing internal membrane sheets (Figure 6A''') [30]. These results are a strong indication that Fgf8 is taken up by target cells via the canonical endocytic pathway and routed to lysosomes, where it is eventually degraded.

The restrictive clearance model further predicts that *RN-tre*-expressing cells that would normally respond with extreme sensitivity to the endogenous Fgf8 levels, regardless of the cells' distance from the Fgf8 source, should nevertheless be sensitive to the presence of (unmanipulated) wild-type cells with normal levels of endocytosis in the intervening space because such wild-type cells might be able to “mop up” Fgf8 protein. To test this prediction, we transplanted small clones of *RN-tre*-overexpressing cells into a host embryo (Figure 6B). Note that we indirectly determine in these experiments the response to the endogenous Fgf8 source and level; direct detection of endogenous Fgf8 protein has so far not been successful. In the first set of experiments, we

implanted the cells close to the source of Fgf8 at the blastoderm margin. In a second set, the cells were implanted at a distance from the source, into the animal pole region. At 60% epiboly, the embryos were analyzed with a probe against the target gene *spry4*. Clones located close to the source showed a strong response to Fgf signaling, even stronger than the endogenous expression of *spry4* in the margin (Figures 6C and 6C'). In addition, host cells surrounding the clone were often positive for *spry4* (Figure 6C', yellow arrows), which may reflect a higher level of Fgf8 protein accumulating in the area of the clone. Importantly, clones of cells that are located at a distance from the source did not show any expression of *spry4* (Figures 6D and 6D') although cells in this position are able to respond in embryos when globally injected with *RN-tre* (compare to Figure 3D). Therefore, the wild-type cells located between the Fgf source and the clone block the ability of clones to respond. We suggest that they take up and degrade the Fgf signal emitted from the blastoderm margin and, consequently, prevent the response of cells located at the animal pole.

In summary, our work suggests that Fgf8 operates as a key signaling molecule in vertebrate embryonic development by extracellular diffusion that can be limited by restrictive clearance, an endocytosis-based mechanism of uptake and degradation (Figure 6E). Target tissues employ this mechanism to clear Fgf8 protein and thus restrict its distribution and the spatial array of target gene responses (Figure 6F). It will be interesting to determine whether and how endocytosis functions in other Fgf-dependent signaling events in the embryo, especially where a long-range signaling event is postulated [3]. Although we have not directly addressed the role of Fgf receptors in restrictive clearance, they are likely to be involved because Fgf8 uptake can be decreased by XFD injection (Figure 2), and inactivation of zebrafish *Fgf1* mimics the phenotype of the Fgf8 loss-of-function mutant *acerebellar* [31]. Because restrictive clearance can regulate Fgf8 protein spreading through its availability in extracellular space, additional mechanisms that influence composition of the extracellular matrix or surface availability of receptors are likely to contribute to controlling ligand propagation as well.

In *Drosophila*, Wingless is a different type of morphogen, for which degradation was invoked to explain an asymmetric response to a Wingless source [32]. Unlike Fgf8, Wingless is thought to spread through lipidic particles [33] and signals through a different class of receptors, and it is as yet unknown if degradation influences propagation of the cognate vertebrate Wnt proteins. For Fgf8, a different mechanism for generating an activity gradient has recently been suggested to operate by regulated *Fgf8* mRNA decay [34]. We find that altering the rate of endocytosis has dramatic consequences for protein distribution and target gene response but do not observe altered *Fgf8* mRNA distribution in such embryos. An important feature of the restrictive clearance mechanism proposed here is that it operates at the level of the protein and, thus, ensures a careful control of the potent effects of Fgf8 protein itself. However, the two mechanisms are not mutually exclusive, and both may be employed in different developmental contexts.

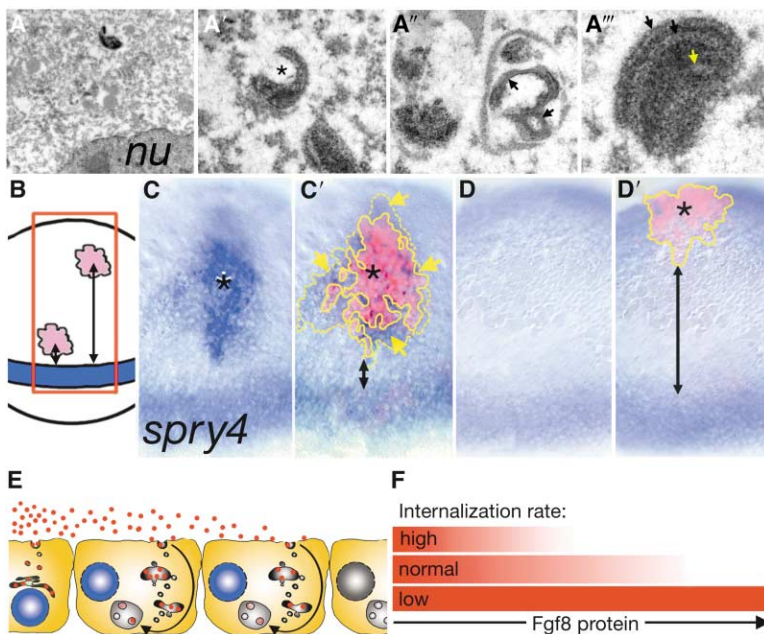


Figure 6. Testing the Restrictive Clearance Model

(A–A''') EM detection of Fgf8:Myc in endosomal structures, including lysosomes, in receiving tissue. An early endosome is marked with a red arrowhead (A). The nucleus and other vesicular structures are visible because of counterstaining. (A') Early endosomes with a typical electron-translucent central part are surrounded by positively stained vacuoles. Inner membranes (black arrows) are positive for Fgf8; the outer membrane surrounding a late endosome/multivesicular body is unlabeled (A''). Labeled lysosomes with internal membrane sheets (arrows) are shown in (A'''). Method: Donor cells from embryos injected with Fgf8:Myc mRNA were heterochronically transplanted at early sphere stage (before onset of *fgf8* expression) into host embryos at 40% epiboly and fixed at 60% epiboly prior to α -Myc antibody staining. Embryos were sectioned and analyzed by electron microscopy at the indicated magnification.

(B–D') Wild-type cells block Fgf8 signal propagation. Donor embryos were injected with 250 pg of *RN-tre* mRNA to decrease endocytosis and coinjected with rhodamine dextran

as lineage tracer (B–D'). At early sphere stage, small cell clones were grafted at different distances from the endogenous, Fgf8-expressing blastoderm margin (B) into embryos at 40% epiboly. At 70%, the embryos were fixed prior to in situ hybridization (ISH) with *spry4* and mounted dorsal to the right. Grafts located close to the source displayed strong staining for *spry4* (C). In addition, wild-type cells surrounding the clones also expressed *spry4*, as shown in the superimposed image (yellow arrows). A solid line surrounds the clone, whereas a dashed yellow line surrounds the halo. An asterisk marks the location of the clone. Black arrows indicate the distance between source tissue and clone. In contrast, cell clones located at a distance from the source tissue did not display *spry4* expression (D). (D) superimposed with the fluorescent image (D') reveals the location of the transplanted cells by the lineage tracer.

(E) Restrictive clearance model: Propagation of Fgf8 protein is limited through clearance from extracellular space by endocytosis and subsequent degradation, effectively restricting the range over which Fgf8 signals in tissue.

(F) Different levels of internalization rates allow different extent of spreading of Fgf8 protein through the target tissue, leading to differential target gene response.

In vertebrates, another TGF- β ligand, Activin, may employ extracellular diffusion to signal during *Xenopus* mesoderm development, although it is unclear whether Activin functions in this process [1]. Gurdon and collaborators suggested that individual cells in a target field can respond to the TGF- β ligand Activin directly, in isolation, and independently of their neighbors by sensing ligand concentration [35]. Our results are entirely consistent with this view. However, we propose that neighboring cells may also influence the availability of Fgf8 ligand to other target cells in an active way, by modulating the degree of destruction and possibly by recycling of the ligand. Tissue culture cells are able to modulate their rate of endocytosis over a wide range, which may change upon exposure to ligand [36]. It will be interesting to determine to what extent rates of endocytosis are modulated in vivo to achieve decisions in development.

Supplemental Data

A Supplemental Figure for this article is available online at <http://www.current-biology.com/cgi/content/full/14/20/1834/DC1>.

Acknowledgments

We thank M. Gonzalez-Gaitan and M. Zerial for discussions, as well as C. Houart, A. Lumsden, A. Oates, M. Zerial and anonymous reviewers for constructive comments on the manuscript; we thank M. Zerial (RN-Tre) and S. Schmid (Dyn2-K44A) for plasmids and D. Stemple for *rab5* morpholinos. This work was supported by the Max

Planck Society and by a grant from the European Union (QLG3-CT-2001-02310).

Received: July 5, 2004

Revised: August 23, 2004

Accepted: August 24, 2004

Published: October 26, 2004

References

- Gurdon, J.B., and Bourillot, P.Y. (2001). Morphogen gradient interpretation. *Nature* 413, 797–803.
- Martinez Arias, A., and Stewart, A. (2002). *Molecular Principles of Animal Development*, First Edition (Oxford: Oxford University Press).
- Scholpp, S., Lohs, C., and Brand, M. (2003). Engrailed and Fgf8 act synergistically to maintain the boundary between diencephalon and mesencephalon. *Development* 130, 4881–4893.
- Meyers, E.N., Lewandoski, M., and Martin, G.R. (1998). An Fgf8 mutant allelic series generated by Cre- and Flp-mediated recombination. *Nat. Genet.* 18, 136–141.
- Reifers, F., Bohli, H., Walsh, E.C., Crossley, P.H., Stainier, D.Y., and Brand, M. (1998). Fgf8 is mutated in zebrafish acerebellar (*ace*) mutants and is required for maintenance of midbrain-hind-brain boundary development and somitogenesis. *Development* 125, 2381–2395.
- Reifers, F., Walsh, E.C., Leger, S., Stainier, D.Y., and Brand, M. (2000). Induction and differentiation of the zebrafish heart requires fibroblast growth factor 8 (*fgf8/acerebellar*). *Development* 127, 225–235.
- Leger, S., and Brand, M. (2002). Fgf8 and Fgf3 are required for zebrafish ear placode induction, maintenance and inner ear patterning. *Mech. Dev.* 119, 91–108.

8. Draper, B.W., Stock, D.W., and Kimmel, C.B. (2003). Zebrafish *fgf24* functions with *fgf8* to promote posterior mesodermal development. *Development* 130, 4639–4654.
9. Citores, L., Wesche, J., Kolpakova, E., and Olsnes, S. (1999). Uptake and intracellular transport of acidic fibroblast growth factor: Evidence for free and cytoskeleton-anchored fibroblast growth factor receptors. *Mol. Biol. Cell* 10, 3835–3848.
10. Furthauer, M., Reifers, F., Brand, M., Thisse, B., and Thisse, C. (2001). *sprouty4* acts in vivo as a feedback-induced antagonist of FGF signaling in zebrafish. *Development* 128, 2175–2186.
11. Zerial, M., and McBride, H. (2001). Rab proteins as membrane organizers. *Nat. Rev. Mol. Cell Biol.* 2, 107–117.
12. Bucci, C., Lutcke, A., Steele-Mortimer, O., Olkkonen, V.M., Dupree, P., Chiariello, M., Bruni, C.B., Simons, K., and Zerial, M. (1995). Co-operative regulation of endocytosis by three Rab5 isoforms. *FEBS Lett.* 366, 65–71.
13. McLauchlan, H., Newell, J., Morrice, N., Osborne, A., West, M., and Smythe, E. (1998). A novel role for Rab5-GDI in ligand sequestration into clathrin-coated pits. *Curr. Biol.* 8, 34–45.
14. Roberts, R.L., Barbieri, M.A., Pryse, K.M., Chua, M., Morisaki, J.H., and Stahl, P.D. (1999). Endosome fusion in living cells overexpressing GFP-rab5. *J. Cell Sci.* 112, 3667–3675.
15. Pauls, S., Geldmacher-Voss, B., and Campos-Ortega, J.A. (2001). A zebrafish histone variant H2A.F/Z and a transgenic H2A.F/Z:GFP fusion protein for in vivo studies of embryonic development. *Dev. Genes Evol.* 211, 603–610.
16. Amaya, E., Stein, P.A., Musci, T.J., and Kirschner, M.W. (1993). FGF signalling in the early specification of mesoderm in *Xenopus*. *Development* 118, 477–487.
17. Sorokin, A., Mohammadi, M., Huang, J., and Schlessinger, J. (1994). Internalization of fibroblast growth factor receptor is inhibited by a point mutation at tyrosine 766. *J. Biol. Chem.* 269, 17056–17061.
18. Levkowitz, G., Waterman, H., Zamir, E., Kam, Z., Oved, S., Langdon, W.Y., Beguinot, L., Geiger, B., and Yarden, Y. (1998). c-Cbl/Sli-1 regulates endocytic sorting and ubiquitination of the epidermal growth factor receptor. *Genes Dev.* 12, 3663–3674.
19. Lanzetti, L., Rybin, V., Malabarba, M.G., Christoforidis, S., Scita, G., Zerial, M., and Di Fiore, P.P. (2000). The Eps8 protein coordinates EGF receptor signalling through Rac and trafficking through Rab5. *Nature* 408, 374–377.
20. Stenmark, H., Parton, R.G., Steele-Mortimer, O., Lutcke, A., Gruenberg, J., and Zerial, M. (1994). Inhibition of rab5 GTPase activity stimulates membrane fusion in endocytosis. *EMBO J.* 13, 1287–1296.
21. Moriyoshi, K., Richards, L.J., Akazawa, C., O’Leary, D.D., and Nakanishi, S. (1996). Labeling neural cells using adenoviral gene transfer of membrane-targeted GFP. *Neuron* 16, 255–260.
22. Entchev, E.V., Schwabedissen, A., and Gonzalez-Gaitan, M. (2000). Gradient formation of the TGF-beta homolog Dpp. *Cell* 103, 981–991.
23. Gonzalez-Gaitan, M. (2003). Signal dispersal and transduction through the endocytic pathway. *Nat. Rev. Mol. Cell Biol.* 4, 213–224.
24. Furthauer, M., Thisse, C., and Thisse, B. (1997). A role for FGF-8 in the dorsoventral patterning of the zebrafish gastrula. *Development* 124, 4253–4264.
25. Raible, F., and Brand, M. (2001). Tight transcriptional control of the ETS domain factors *Erm* and *Pea3* by Fgf signaling during early zebrafish development. *Mech. Dev.* 107, 105–117.
26. Roehl, H., and Nusslein-Volhard, C. (2001). Zebrafish *pea3* and *erm* are general targets of FGF8 signaling. *Curr. Biol.* 11, 503–507.
27. Mohammadi, M., McMahon, G., Sun, L., Tang, C., Hirth, P., Yeh, B.K., Hubbard, S.R., and Schlessinger, J. (1997). Structures of the tyrosine kinase domain of fibroblast growth factor receptor in complex with inhibitors. *Science* 276, 955–960.
28. van der Bliek, A.M., Redelmeier, T.E., Damke, H., Tisdale, E.J., Meyerowitz, E.M., and Schmid, S.L. (1993). Mutations in human dynamin block an intermediate stage in coated vesicle formation. *J. Cell Biol.* 122, 553–563.
29. Sachse, M., Ramm, G., Strous, G., and Klumperman, J. (2002). Endosomes: Multipurpose designs for integrating housekeeping and specialized tasks. *Histochem. Cell Biol.* 117, 91–104.
30. Kleijmeer, M.J., Morkowski, S., Griffith, J.M., Rudensky, A.Y., and Geuze, H.J. (1997). Major histocompatibility complex class II compartments in human and mouse B lymphoblasts represent conventional endocytic compartments. *J. Cell Biol.* 139, 639–649.
31. Scholpp, S., Groth, C., Lohs, C., Lardelli, M., and Brand, M. (2004). Zebrafish *fgf1* is a member of the *fgf8* synexpression group and is required for *fgf8* signalling at the midbrain-hind-brain boundary. *Dev. Genes Evol.*, in press.
32. Dubois, L., Lecourtois, M., Alexandre, C., Hirst, E., and Vincent, J.P. (2001). Regulated endocytic routing modulates wingless signaling in *Drosophila* embryos. *Cell* 105, 613–624.
33. Greco, V., Hannus, M., and Eaton, S. (2001). Argosomes: A potential vehicle for the spread of morphogens through epithelia. *Cell* 106, 633–645.
34. Dubrulle, J., and Pourquie, O. (2004). *fgf8* mRNA decay establishes a gradient that couples axial elongation to patterning in the vertebrate embryo. *Nature* 427, 419–422.
35. Bourillot, P.Y., Garrett, N., and Gurdon, J.B. (2002). A changing morphogen gradient is interpreted by continuous transduction flow. *Development* 129, 2167–2180.
36. Mellman, I. (1996). Endocytosis and molecular sorting. *Annu. Rev. Cell Dev. Biol.* 12, 575–625.
37. Cooper, M.S., D’Amico, L.A., and Henry, C.A. (1999). Confocal microscopic analysis of morphogenetic movements. *Methods Cell Biol.* 59, 179–204.